Journal of Human Genetics
(JHG-19-001 revised MS)

Gene regulation by antitumor *miR-130b-5p* in pancreatic ductal adenocarcinoma: the clinical significance of oncogenic *EPS8*

Haruhi Fukuhisa[1], Naohiko Seki[2], Tetsuya Idichi[1], Hiroshi Kurahara[1], Yasutaka Yamada[2], Hiroko Toda[1], Yoshiaki Kita[1], Yota Kawasaki[1], Kiyonori Tanoue[1], Yuko Mataki[1], Kosei Maemura[1], Shoji Natsugoe[1]

[1] Department of Digestive Surgery, Breast and Thyroid Surgery, Graduate School of Medical and Dental Sciences, Kagoshima University, Kagoshima, Japan
[2] Department of Functional Genomics, Chiba University Graduate School of Medicine, Chiba, Japan

Running title: Regulation of *EPS8* by antitumor *miR-130b-5p* in PDAC

Correspondence to:
Naohiko Seki, Ph.D.
Associate Professor of Functional Genomics
Department of Functional Genomics
Chiba University Graduate School of Medicine
1-8-1 Inohana Chuo-ku, Chiba 260-8670, Japan
Tel: +81-43-226-2971
Fax: +81-43-227-3442
E-mail: naoseki@faculty.chiba-u.jp

Abstract

Our ongoing analyses identifying dysregulated microRNAs (miRNAs) and their controlled target RNAs have shed light on novel oncogenic pathways in pancreatic ductal adenocarcinoma (PDAC). The PDAC miRNA signature obtained by RNA sequencing showed that both strands of pre-*miR-130b* (*miR-130b-5p*, the passenger strand and *miR-130b-3p*, the guide strand) were significantly downregulated in cancer tissues. Our functional assays revealed that *miR-130b-5p* significantly blocked the malignant abilities of PDAC cell lines (PANC-1 and SW1990), e.g., cancer cell proliferation, migration and invasion. A total of 103 genes were identified as possible oncogenic targets by *miR-130b-5p* regulation in PDAC cells based on genome-wide gene expression analysis and *in silico* database search. Among the possible targets, high expression of 9 genes (*EPS8*, *ZWINT*, *SMC4*, *LDHA*, *GJB2*, *ZCCHC24*, *TOP2A*, *ANLN* and *ADCY3*) predicted a significantly poorer prognosis of PDAC patients (5-year overall survival, $p < 0.001$). Furthermore, we focused on *EPS8* because its expression had the greatest impact on patient prognosis (overall survival, $p < 0.0001$). Overexpression of *EPS8* was detected in PDAC clinical specimens. Knockdown assays with si*EPS8* showed that its overexpression enhanced cancer cell proliferation, migration and invasion. Analysis of downstream RNA networks regulated by *EPS8* indicated that *MET*, *HMGA2*, *FERMT1*, *RARRES3*, *PTK2*, *MAD2L1* and *FLI1* were closely involved in PDAC pathogenesis. Genes regulated by antitumor *miR-130b-5p* were closely involved in PDAC molecular pathogenesis. Our approach, discovery of antitumor miRNAs and their target RNAs, will contribute to exploring the causes of this malignant disease.

Keywords: microRNA, passenger strand, *miR-130b-5p*, pancreatic ductal adenocarcinoma, *EPS8*, antitumor

Introduction

Due to a lack of early diagnostic strategies and its aggressive nature, pancreatic ductal adenocarcinoma (PDAC) is one of the most lethal cancers known to medicine [1]. Treatment options for locally advanced or metastatic PDAC are limited, and the median life expectancy is 6–11 months and 3–6 months for patients presenting with locally advanced disease or metastatic disease, respectively [2, 3]. Searching for new therapeutic targets and developing useful prognostic molecular markers are important goals to improve treatment outcomes of PDAC.

MicroRNAs (miRNAs) are small noncoding RNAs 19–24 nucleotides in length. They regulate gene expression by repressing translation or by cutting mRNAs in a sequence-dependent manner [4-6]. A single miRNA species is capable of modulating many protein-coding and noncoding RNA transcripts [7-9]. Thus, aberrantly expressed miRNAs can disrupt normal cell function, including supporting cancer pathogenesis [7-9].

Based on our original miRNA expression signatures by current genomic approaches, including that for PDAC, we have identified RNA networks that are controlled by antitumor miRNAs in several cancers [10-15]. In PDAC cells, our previous studies demonstrated that *miR-375*, *miR-216b-3p*, *miR-217*, *miR-148a* and *miR-124-3p* were downregulated in PDAC tissues and these miRNAs had tumor suppressing functions, including controlling various oncogenes in PDAC cells [14, 16-19].

For example, expression of anillin (*ANLN*), actin-binding protein was directly controlled by *miR-217* and aberrant expression of *ANLN* promoted to cancer cell migration and invasion capabilities of PDAC cell lines [17]. Ectopic expression of *miR-124-3p* attenuated cancer cell aggressiveness through targeting oncogenic signaling via FAK, AKT and ERK in PDAC cells [19]. Integrin α3 (*ITGA3*) and integrin β1 (*ITGB1*) were direct targets of *miR-124-3p* regulation in PDAC cells [19]. These findings suggest that analyses of antitumor miRNAs that regulate RNA networks will enhance understanding of PDAC molecular pathogenesis.

In this study, we focused on the passenger and guide strands of the *miR-130b* duplex *(miR-130b-5p*, the passenger strand and *miR-130b-3p*, the guide strand) based on miRNA expression signature of PDAC by RNA sequencing. Involvement of passenger strands of miRNAs is a new concept of miRNA biogenesis and these miRNAs provide the opportunity to find new regulatory networks in cancer cells. Here, we investigated the antitumor roles of *miR-130b-5p*, and their regulated oncogenic genes in PDAC pathogenesis.

Materials and methods

Human PDAC clinical specimens and cell lines

The present study was approved by the Bioethics Committee of Kagoshima University (Kagoshima, Japan; approval no. 160038 28-65). Written prior informed consent and approval were obtained from all of the patients.

In this study, 31 PDAC clinical samples were collected from PDAC patients who underwent resection at Kagoshima University Hospital from 1997 to 2016. Fifteen normal pancreatic tissue specimens were collected from noncancerous regions. The clinical samples were staged according to the American Joint Committee on Cancer/Union Internationale Contre le Cancer (UICC) TNM classification. Clinical features in PDAC specimens are shown in Supplemental Table 1.

We used two PDAC cell lines: SW1990, purchased from the American Type Culture Collection (Manassas, VA, USA), and PANC-1, purchased from RIKEN Cell Bank (Tsukuba, Ibaraki, Japan).

Quantitative real-time reverse transcription polymerase chain reaction (qRT-PCR)

The procedure for qRT-PCR has been described previously [17-21]. TaqMan qRT-PCR probes were obtained from Thermo Fisher Scientific(Waltham, MA, USA) as follows: *miR-130b-5p* (product ID: 002114), *miR-130b-3p* (product ID: 00456) and *EPS8* (product ID: Hs00610286_mH). *GUSB* (product ID: Hs99999908_m1) and *RNU48*

(product ID: 001006) were used as internal controls.

Transfection of mimic and inhibitor miRNA, small interfering RNA (siRNA) into PDAC cells

The following mature miRNAs and siRNAs were transfected into PDAC cells (PANC-1 and SW1990): *miR-130b-5p* (product ID: PM12970, Applied Biosystems, Foster City, CA, USA), *miR-130b-3p* (product ID: PM10777, Applied Biosystems) and Stealth Select RNAi siRNA, *EPS8* siRNAs (product IDs: HSS103325 and HSS103326, Invitrogen, Carlsbad, CA, USA). The transfection procedures were described in previous studies [20-25].

Incorporation of *miR-130b-5p* into the RISC: assessment by Ago2 immunoprecipitation

Agonaute-2 (Ago2) is an essential components of the RNA-induced silencing complex (RISC) that binds to miRNAs. miRNAs were transfected into PANC-1 cells and were isolated using a microRNA Isolation Kit, Human Ago2 (Wako Pure Chemical Industries, Ltd., Osaka, Japan) as described previously [22-24]. The expression levels of Ago2-conjugated miRNAs were assessed by qRT-PCR assay.

Cell proliferation, migration and invasion assays

Functional assays for determining cell proliferation, migration, and invasion were described previously [16-19].

Identification of putative oncogenic target genes regulated by *miR-130b-5p* in PDAC cells

To identify *miR-130b-5p*-controlled oncogenes, the following data sets were used: genome-wide gene expression analyses using PDAC cells transfected with *miR-130b-5p* predicted putative target genes that have *miR-130b-5p* binding sites in their 3′ untranslated regions (TargetScan database ver. 7.1) and gene expression data of PDAC clinical specimens (Gene Expression Omnibus dataset: GEO accession number, GSE15471). Gene expression data (*miR-130b-5p* transfected PANC-1 cells) were

deposited into the GEO database (accession number: GSE115801). An outline of the approach is shown in Supplemental Figure 1 and was described in previous studies [20-25].

Exploration of downstream targets regulated by si-*EPS8* in PDAC cells

Genome-wide gene expression and database oriented *in silico* analyses were applied to identify *EPS8*-mediated downstream genes. Outlines of the strategies were described in our previous studies [17, 18, 20, 21]. Our target search strategy in this study is shown in Supplemental Figure 2. Gene expression data were deposited in GEO database (accession number: GSE118966).

PDAC clinical data analysis by TCGA database

TCGA database was used to investigate the clinical significance of PDAC miRNAs and the genes they regulated (https://tcga-data.nci.nih.gov/tcga/). Gene expression and clinical data were obtained from cBioPortal (http://www.cbioportal.org/) and OncoLnc (http://www.oncolnc.org) (data downloaded on April 28, 2018). Detailed information on the databases were described in the previous papers [26-28].

Western blot analysis and Immunohistochemistry

The procedures for Western blotting and immunohistochemistry were described in previous studies [17-19]. These assays used the following antibodies: anti-EPS8 (product ID: #43114, Cell Signaling Technology, Danvers, MA, USA) and anti-GAPDH (product ID: SAF6698, Wako).

Tissue sections were incubated overnight at 4˚C with anti-EPS8 antibodies diluted 1:400 (HPA003897; Sigma- Aldrich, St. Louis, MO, USA).

Luciferase reporter assays

The following 2 sequences were cloned into the psiCHECk-2 vector (C8021; Promega Corporation, Madison, WI, USA): the

wild-type sequence of the 3'-untranslated regions (UTRs) of *EPS8*, or the deletion-type, which lacked the *miR-130b-5p* target sites from *EPS8* (position 713-719). The procedures for transfection and dual-luciferase reporter assays were provided in previous studies [20-25].

Statistical analysis

To assess the significance of differences between 2 groups, we used Mann-Whitney *U* tests. Differences between multiple groups were assessed by one-way ANOVA and Tukey tests for post-hoc analysis. We evaluated the correlations between the expression levels of *miR-130b-5p* and *EPS8* using Spearman's rank test. Tests utilized Expert StatView version 5.0 (SAS Institute, Inc., Cary, NC, USA) and JMPPro 14.0.0 (SAS Institute, Inc., Cary, NC, USA).

Results

Downregulation of *miR-130b-5p* and *miR-130b-3p* in PDAC clinical specimens and cell lines

We performed qRT-PCR to evaluate the expression levels of *miR-130b-5p* and *miR-130b-3p* in PDAC tissues (n = 31) as well as in normal pancreatic tissues (n = 15) and in 2 PDAC cell lines (PANC-1 and SW1990). Clinical features of the patients are summarized in Supplemental Table 1.

The expression levels of *miR-130b-5p* and *miR-130b-3p* were significantly downregulated in cancer tissues ($p = 0.0005$ and $p = 0.0009$; Figure. 1A). Spearman’s rank test showed a positive correlation between the expression levels of *miR-130b-5p* and *miR-130b-3p* ($p < 0.0001$, $r = 0.875$; Figure 1B).

In 2 cancer cell lines, PANC-1 and SW1990, the expression levels of *miR-130b-5p* and *miR-130b-3p* were extremely low (Figure 1A).

Effects of ectopic expression of *miR-130b-5p* and *miR-130b-3p* on PDAC cells

To verify the antitumor roles of *miR-130b-5p* and *miR-130b-3p*, we conducted gain-of-function studies by miRNA transfection into PANC-1 and SW1990 cells.

In cell proliferation assays, the inhibition of cancer cell growth was only detected with *miR-130b-5p* transfection into PANC-1 cells (Figure 1C). Cell migration activities were reduced in the cells transfected with *miR-130b-5p* or *miR-130b-3p* (Figure 1D).

Matrigel invasion assays revealed that transfection with *miR-130b-5p* or *miR-130b-3p* significantly decreased cell invasive capacity (Figure 1E). However, no change was observed in *miR-130b-3p* transfection into PANC-1 cells (Figure 1E).

Incorporation of *miR-130b-5p* and *miR-130b-3p* into the RISC in PDAC cells

Ago2 is an essential component of the RISC. We hypothesized that the *miR-130b-3p* passenger strand in PDAC cells might be incorporated into the RISC where it could act as a tumor suppressor. To test that possibility, Ago2 was immunoprecipitated from PANC-1 cells that had been transfected with either *miR-130b-5p* or *miR-130b-3p*. Following isolation of Ago2-bound miRNAs, they were analyzed by qRT-PCR to determine whether *miR-130b-5p* or *miR-130b-3p* or both were associated. In transfectants, we observed higher levels of *miR-130-5p* expression than in mock transfectants or miR-controls or *miR-130b-3p* ($p < 0.005$) (Supplemental Figure 3).

Identification of putative target genes controlled by *miR-130b-5p* in PDAC cells

To predict putative target genes controlled by *miR-130b-5p* in PDACs, we combined data from the following: genome-wide gene expression data (miR-*130b-5p* transfected into PANC-1 cells; GEO accession number: GSE115801), gene expression data from PDAC clinical specimens (GSE15471) and TargetScan database. The selection strategy of *miR-130b* targets is shown in Supplemental Figure 1. A total of 103 genes were identified as putative *miR-*

130b-5p controlled oncogenes in PDAC cells (Table 1).

To investigate the relationship between these target genes and the course of PDAC, we examined these genes with TCGA database. Among these targets, high expression of 9 genes (*EPS8*, *ZWINT*, *SMC4*, *LDHA*, *GJB2*, *ZCCHC24*, *TOP2A*, *ANLN* and *ADCY3*) was associated with poor prognosis (5-year overall survival rates: $p < 0.01$) (Figure 2).

Below, we focused on *EPS8* (epidermal growth factor receptor kinase substrate 8) because its expression was the most significantly predicted poor prognosis of the PDAC patients (Table 2, Figure 2).

Expression of *EPS8* in PDAC clinical specimens and its clinical significance

The levels of *EPS8* mRNA were significantly upregulated in PDAC tissues (Figure 3A), with a negative correlation between the expression of *EPS8* and *miR-130b-5p* ($p = 0.0191$, $r = -0.349$; Spearman's rank tests, Figure 3B).

Cox hazard regression analyses assessed the clinical significance of *EPS8* expression for OS in patients with PDAC. With multivariate analysis, we found that *EPS8* expression was an independent predictive factor for OS (hazard ratio = 1.893, $p = 0.0053$; Figure 3C).

PDAC clinical specimens were subjected to immunohistochemical analyses. The results indicated that EPS8 protein was strongly expressed in cancer lesions. In contrast, expression was infrequent and weak in normal pancreatic cells (Figure 3D).

Direct regulation of *EPS8* by *miR-130b-5p* in PDAC cells

In cells transfected with *miR-130b-5p,* the levels of *EPS8* mRNA and EPS8 protein were significantly lower than mock- or miR-control-transfected cells (Figures 4A and 4B). Binding sites for *miR-130b-5p* in the 3'-UTR of *EPS8* (positions 713-719, Figures 4C, upper) were predicted by the TargetScan database. We used luciferase reporter assays with vectors carrying either the

wild-type or deletion-type 3'-UTR of *EPS8*. We observed greatly reduced luminescence after transfection with *miR-130b-5p* and the vector carrying the wild-type 3′-UTR of *EPS8*. Transfection with the deletion-type vector did not reduce luminescence intensities in PANC-1 and SW1990 cells. Thus, *miR-130b-5p* directly bound to *EPS8* in the 3′-UTR (Figure 4C).

In addition, we investigated the effect of suppression of *EPS8*/EPS8 by *miR-130a-5p* (seed sequence is almost identical) in PDAC cells. Expression of *EPS8*/EPS8 was slightly suppressed by *miR-130a-5p* in PANC-1 and SW1990 (data not shown).

Effects of silencing *EPS8* on PDAC cells

Next, we transfected siRNAs into PANC-1 and SW1990 cells to examine the function of *EPS8* in PDAC cells. The mRNA and protein expression levels of *EPS8*/EPS8 were decreased by si-*EPS8* (Supplemental Figures 4A and 4B).

We examined the effects of knockdown of *EPS8* in PDAC cells, and found that cell proliferation was not affected (Figure 4D). Cancer cell migration and invasive activities were significantly inhibited by si-*EPS8* transfection into PDAC cells, PANC-1 and SW1990. However, silencing of *EPS8* did not affect cell proliferation (Figures 4D-4F).

Downstream genes affected by silencing of *EPS8* in PDAC cells

To identity downstream genes controlled by *EPS8*, we used two sets of genome-wide gene expression data (si-*EPS8* transfected cells: GSE118966 and PDAC expression data: GSE15471). Our selection strategy is shown in Supplemental Figure 2.

In total, 48 genes were identified as putative downstream genes controlled by *EPS8* in PDAC cells (Table 2). Among 8 genes, high expression affected overall survival rates ($p < 0.05$). Specifically, *MET*, *HMGA2*, *CORO1C*, *FERMT1*, *RARRES3*, *PTK2*, *MAD2L1* and *FLI1* were significantly associated with poor prognosis in patients with PDAC by TCGA analysis (Table 2 and Supplemental Figure 5).

Discussion

miRNAs have unique characteristics. For example, a single miRNA species can regulate vast numbers of RNA transcripts in normal and pathological cells. Expression of RNAs controlled by miRNA varies depending on the cell [7-9]. Therefore, identification of aberrantly expressed miRNAs and their targets is the first step in elucidating molecular pathogenesis in PDAC cells. Using our original miRNA signature of PDAC by RNA sequencing, the molecular network controlled by antitumor miRNAs in PCAD cells is being clarified [14, 16-19]. In this study, we focused on both strands of pre-*miR-130b*(*miR-130b-5p* and *miR-130b-3p*) because these miRNAs were significantly downregulated in our and other PDAC signatures [14, 29, 30].

Several miRNAs form families based on their seed sequences. The *miR-130* family consists of 4 miRNAs: *miR-130a* (chromosome 11q12.1), *miR-130b* (22q11.21), *miR-301a* (17q22) and *miR-301b* (22q11.21) [31-33]. The seed sequences of passenger strands *miR-130a-5p* and *miR-130b-5p* are almost identical. The seed sequences of guide strands of all member of the *miR-130* family (*miR-130a-3p*, *miR-130b-3p*, *miR-301a-3p* and *miR-301b-3p*) are identical (seed sequences are summarized in Supplemental Figure 6). Previous studies showed that a number of *miR-130* family (guide strands) were overexpressed in cancer tissues and their functions were involved in oncogenesis, e.g., bladder cancer, esophageal squamous cell carcinoma and lung cancer [32, 34, 35].

Contrary to these reports, *miR-130a* and *miR-130b* were downregulated in cancer tissues and they acted as antitumor miRNAs in ovarian cancer, prostate cancer, endometrial cancer and papillary thyroid carcinoma [36, 37]. Our present data shows that both strands (*miR-130b-5p* and *miR-130b-3p)* were significantly reduced in PDAC clinical specimens and cell lines. Furthermore, ectopic expression of these miRNAs inhibited malignant phenotypes in PDAC cells, suggesting that both *miR-130b-5p* and *miR-130b-3p* play antitumor roles in PDAC cells. In a previous study of PDAC cells, expression of *miR-130b-3p* was

suppressed in cancer tissues and its expression was an independent prognostic predictor of the patients' disease course [38]. Overexpression of *miR-130b-3p* induced apoptotic cells through targeting of *STAT3* in PDAC cells [38]. These findings showed that *miR-130b* has multiple functions, oncogenic or antitumor roles depending on the specific cancer cell. It is indispensable to elucidate the molecular mechanism controlling *miR-130b* expression in several types of cancer cells.

Previous study showed that hyper-methylation of promoter region of *miR-130b* was observed in ovarian cancer clinical tissues and cell lines and methylation cased to downregulation of *miR-130b* expression [31, 33]. In prostate cancer, downregulation of *miR-130b*/*miR-301b* cluster was detected in clinical specimens and cell lines [31, 33]. Methylation levels of their promoter region was significantly higher in prostate cancer tissues compared to normal tissues [31, 33]. Expression levels of *miR-130b* and *miR-301b* were upregulated by treatment of demethylation drugs [31, 33]. These findings showed that downregulation of *miR-130b* was mediated by aberrant methylation on its promoter region. For *miR-130* family, comprehensive analysis of the molecular mechanism of suppressing their expression in PDAC cells is indispensable.

This is the first report that *miR-130b-5p* (the passenger strand) acted as an antitumor miRNA in PDAC. Therefore, we focused on *miR-130b-5p* to investigate its control of oncogenes involved in PDAC pathogenesis. In this study, a total of 103 putative oncogenes were identified that were regulated by *miR-130b-5p* in PDAC cells. Among these targets, overexpression of 9 genes (*EPS8*, *ZWINT*, *SMC4*, *LDHA*, *GJB2*, *ZCCHC24*, *TOP2A*, *ANLN* and *ADCY3*) were closely associated with poor prognosis of the patients with PDAC. Interestingly, aberrant expression of *ANLN* (actin-binding protein anillin) was detected in PDAC clinical specimens [17]. Knockdown assays of *ANLN* expression markedly inhibited cancer cell migration and invasive capabilities of PDAC cell lines [17]. In addition, *ANLN* was directly controlled byantitumor *miR-217* in PDAC cells [17].

Furthermore, we investigated the functional significance of *EPS8* (epidermal growth factor receptor pathway substrate 8) in PDAC cells. EPS8 binds several adaptor proteins and acts as a substrate for receptor and non-receptor tyrosine kinases, e.g., EGFR, FGFR, VEGFR and Src [39]. Other studies showed that *EPS8* has actin-binding ability and it acts by capping barbed ends and promoting bundling [40]. Furthermore, EPS8 forms a trimer (EPS8, Abi-1 and SOS-1) and this complex acts as a guanine nucleotide exchange factor (GEFs) in Rac signaling and contributes to Rac-based actin polymerizing processes [41]. Aberrantly expressed *EPS8* was reported in colon cancer, breast cancer, hematologic malignancies and cervical cancer, and its overexpression was closely involved in the malignant phenotype [42-45]. Our present data revealed that *EPS8* regulated cancer cell migration and invasion and its expression is promising as a diagnostic marker for PDAC. Aberrant expression of *EPS8* might be a promising therapeutic target for PDAC.

Finally, to investigate the *EPS8*-mdiated oncogenic genes and pathways in PDAC cells, we applied genome-wide gene expression analyses using knockdown of *EPS8* in cells. A total of 48 genes were identified as putative *EPS8*-mediated targets in PDAC cells. Surprisingly, aberrant expression of 7 genes (*MET*, *HMGA2*, *FERMT1*, *RARRES3*, *PTK2*, *MAD2L1* and *FLI1*, $p < 0.05$) was closely associated with poor prognosis of patients with PADC. In this study, it was revealed that many of the genes controlled by antitumor *miR-130b-5p* and *ESP8*-mediated downstream genes were closely involved in the molecular pathogenesis of PDAC. Elucidation of novel RNA networks controlled by antitumor miRNAs will accelerate comprehensive understanding of molecular pathogenesis of PDAC.

In conclusion, our results showed that expression of both strands of the pre-*miR-130b* duplex were significantly downregulated in PDAC clinical specimens and thus the *miR-130b*-duplex could act as an antitumor miRNA in such cells. A total of 9 genes (*EPS8*, *ZWINT*, *SMC4*, *LDHA*, *GJB2*, *ZCCHC24*, *TOP2A*, *ANLN* and *ADCY3*) were closely associated with PDAC pathogenesis. Among

these targets, aberrant expression of *EPS8* enhanced cancer aggressiveness, suggesting that *EPS8* could be a promising therapeutic target for PDAC. Our approach, discovery of antitumor miRNAs and their target RNAs, will contribute to exploring the causes of this malignant disease.

Acknowledgment

This study was supported by Japan Society for the Promotion of Science 17H04285, 18K08626, 18K08687, 18K16322, 18K09338, 16K19945, and 18K15219.

Conflict of Interest

Authors declare no conflicts of interest for this article

References

1. Kamisawa T, Wood LD, Itoi T, Takaori K. Pancreatic cancer. Lancet. 2016;388:73-85.
2. Das S, Batra SK. Pancreatic cancer metastasis: are we being pre-EMTed? Curr Pharm Des. 2015;21:1249-55.
3. Polireddy K, Chen Q. Cancer of the Pancreas: Molecular Pathways and Current Advancement in Treatment. J Cancer. 2016;7:1497-514.
4. Bartel DP. MicroRNAs: genomics, biogenesis, mechanism, and function. Cell. 2004;116:281-97.
5. Bartel DP. MicroRNAs: target recognition and regulatory functions. Cell. 2009;136:215-33.
6. Liu WW, Meng J, Cui J, Luan YS. Characterization and Function of MicroRNA(*)s in Plants. Frontiers in plant science. 2017;8:2200.
7. Goto Y, Kurozumi A, Enokida H, Ichikawa T, Seki N. Functional significance of aberrantly expressed microRNAs in prostate cancer. Int J Urol. 2015;22:242-52.
8. Koshizuka K, Hanazawa T, Arai T, Okato A, Kikkawa N, Seki N. Involvement of aberrantly expressed microRNAs in the pathogenesis of head and neck squamous cell carcinoma. Cancer Metastasis Rev. 2017;36:525-45.
9. Yonemori K, Kurahara H, Maemura K, Natsugoe S. MicroRNA in pancreatic cancer. J Hum Genet. 2017;62:33-40.
10. Itesako T, Seki N, Yoshino H, Chiyomaru T, Yamasaki T, Hidaka H, et al. The microRNA expression signature of bladder cancer by deep sequencing: the functional significance of the miR-195/497 cluster. PLoS One. 2014;9:e84311.
11. Goto Y, Kurozumi A, Arai T, Nohata N, Kojima S, Okato A, et al. Impact of novel miR-145-3p regulatory networks on survival in patients with castration-resistant prostate cancer. Br J Cancer. 2017;117:409-20.
12. Koshizuka K, Nohata N, Hanazawa T, Kikkawa N, Arai T, Okato A, et al. Deep sequencing-based microRNA expression signatures in head and neck squamous cell carcinoma: dual strands of pre-miR-150 as antitumor miRNAs. Oncotarget. 2017;8:30288-304.
13. Mizuno K, Mataki H, Arai T, Okato A, Kamikawaji K, Kumamoto T, et al. The microRNA expression signature of small cell lung cancer: tumor suppressors of miR-27a-5p and miR-34b-3p and their targeted oncogenes. J Hum Genet. 2017;62:671-78.
14. Yonemori K, Seki N, Idichi T, Kurahara H, Osako Y, Koshizuka K, et al. The

microRNA expression signature of pancreatic ductal adenocarcinoma by RNA sequencing: anti-tumour functions of the microRNA-216 cluster. Oncotarget. 2017;8:70097-115.

15. Toda H, Kurozumi S, Kijima Y, Idichi T, Shinden Y, Yamada Y, et al. Molecular pathogenesis of triple-negative breast cancer based on microRNA expression signatures: antitumor miR-204-5p targets AP1S3. J Hum Genet. 2018;63:1197-210.
16. Yonemori K, Seki N, Kurahara H, Osako Y, Idichi T, Arai T, et al. ZFP36L2 promotes cancer cell aggressiveness and is regulated by antitumor microRNA-375 in pancreatic ductal adenocarcinoma. Cancer Sci. 2017;108:124-35.
17. Idichi T, Seki N, Kurahara H, Yonemori K, Osako Y, Arai T, et al. Regulation of actin-binding protein ANLN by antitumor miR-217 inhibits cancer cell aggressiveness in pancreatic ductal adenocarcinoma. Oncotarget. 2017;8:53180-93.
18. Idichi T, Seki N, Kurahara H, Fukuhisa H, Toda H, Shimonosono M, et al. Molecular pathogenesis of pancreatic ductal adenocarcinoma: Impact of passenger strand of pre-miR-148a on gene regulation. Cancer Sci. 2018;109:2013-26.
19. Idichi T, Seki N, Kurahara H, Fukuhisa H, Toda H, Shimonosono M, et al. Involvement of anti-tumor miR-124-3p and its targets in the pathogenesis of pancreatic ductal adenocarcinoma: direct regulation of ITGA3 and ITGB1 by miR-124-3p. Oncotarget. 2018;9:28849-65.
20. Yamada Y, Arai T, Sugawara S, Okato A, Kato M, Kojima S, et al. Impact of novel oncogenic pathways regulated by antitumor miR-451a in renal cell carcinoma. Cancer Sci. 2018;109:1239-53.
21. Yamada Y, Sugawara S, Arai T, Kojima S, Kato M, Okato A, et al. Molecular pathogenesis of renal cell carcinoma: Impact of the anti-tumor miR-29 family on gene regulation. Int J Urol. 2018;25:953-65.
22. Osako Y, Seki N, Koshizuka K, Okato A, Idichi T, Arai T, et al. Regulation of SPOCK1 by dual strands of pre-miR-150 inhibit cancer cell migration and invasion in esophageal squamous cell carcinoma. J Hum Genet. 2017;62:935-44.
23. Sugawara S, Yamada Y, Arai T, Okato A, Idichi T, Kato M, et al. Dual strands of the miR-223 duplex (miR-223-5p and miR-223-3p) inhibit cancer cell aggressiveness: targeted genes are involved in bladder cancer pathogenesis. J Hum Genet. 2018;63:657-68.
24. Yamada Y, Arai T, Kojima S, Sugawara S, Kato M, Okato A, et al. Regulation of antitumor miR-144-5p targets oncogenes: Direct regulation of syndecan-3 and its clinical significance. Cancer Sci. 2018;109:2919-36.
25. Arai T, Kojima S, Yamada Y, Sugawara S, Kato M, Yamazaki K, et al. Pirin: a

potential novel therapeutic target for castration-resistant prostate cancer regulated by miR-455-5p. Mol Oncol. 2019;13:322-37.

26. Cerami E, Gao J, Dogrusoz U, Gross BE, Sumer SO, Aksoy BA, et al. The cBio cancer genomics portal: an open platform for exploring multidimensional cancer genomics data. Cancer Discov. 2012;2:401-4.
27. Gao J, Aksoy BA, Dogrusoz U, Dresdner G, Gross B, Sumer SO, et al. Integrative analysis of complex cancer genomics and clinical profiles using the cBioPortal. Science signaling. 2013;6:pl1.
28. Anaya J. OncoLnc: linking TCGA survival data to mRNAs, miRNAs, and lncRNAs. PeerJ Computer Science. 2016;2:e67.
29. Mah SM, Buske C, Humphries RK, Kuchenbauer F. miRNA*: a passenger stranded in RNA-induced silencing complex? Crit Rev Eukaryot Gene Expr. 2010;20:141-8.
30. Yang J, Zeng Y. Identification of miRNA-mRNA crosstalk in pancreatic cancer by integrating transcriptome analysis. Eur Rev Med Pharmacol Sci. 2015;19:825-34.
31. Yang C, Cai J, Wang Q, Tang H, Cao J, Wu L, et al. Epigenetic silencing of miR-130b in ovarian cancer promotes the development of multidrug resistance by targeting colony-stimulating factor 1. Gynecol Oncol. 2012;124:325-34.
32. Egawa H, Jingushi K, Hirono T, Ueda Y, Kitae K, Nakata W, et al. The miR-130 family promotes cell migration and invasion in bladder cancer through FAK and Akt phosphorylation by regulating PTEN. Sci Rep. 2016;6:20574.
33. Ramalho-Carvalho J, Graca I, Gomez A, Oliveira J, Henrique R, Esteller M, et al. Downregulation of miR-130b~301b cluster is mediated by aberrant promoter methylation and impairs cellular senescence in prostate cancer. J Hematol Oncol. 2017;10:43.
34. Yu T, Cao R, Li S, Fu M, Ren L, Chen W, et al. MiR-130b plays an oncogenic role by repressing PTEN expression in esophageal squamous cell carcinoma cells. BMC Cancer. 2015;15:29.
35. Zhang Q, Zhang B, Sun L, Yan Q, Zhang Y, Zhang Z, et al. MicroRNA-130b targets PTEN to induce resistance to cisplatin in lung cancer cells by activating Wnt/beta-catenin pathway. Cell Biochem Funct. 2018;36:194-202.
36. Dong P, Karaayvaz M, Jia N, Kaneuchi M, Hamada J, Watari H, et al. Mutant p53 gain-of-function induces epithelial-mesenchymal transition through modulation of the miR-130b-ZEB1 axis. Oncogene. 2013;32:3286-95.
37. Dettmer MS, Perren A, Moch H, Komminoth P, Nikiforov YE, Nikiforova MN. MicroRNA profile of poorly differentiated thyroid carcinomas: new diagnostic and prognostic insights. J Mol Endocrinol. 2014;52:181-9.

38. Zhao G, Zhang JG, Shi Y, Qin Q, Liu Y, Wang B, et al. MiR-130b is a prognostic marker and inhibits cell proliferation and invasion in pancreatic cancer through targeting STAT3. PLoS One. 2013;8:e73803.
39. Fazioli F, Minichiello L, Matoska V, Castagnino P, Miki T, Wong WT, et al. Eps8, a substrate for the epidermal growth factor receptor kinase, enhances EGF-dependent mitogenic signals. EMBO J. 1993;12:3799-808.
40. Logue JS, Cartagena-Rivera AX, Baird MA, Davidson MW, Chadwick RS, Waterman CM. Erk regulation of actin capping and bundling by Eps8 promotes cortex tension and leader bleb-based migration. eLife. 2015;4:e08314.
41. Chen H, Wu X, Pan ZK, Huang S. Integrity of SOS1/EPS8/ABI1 tri-complex determines ovarian cancer metastasis. Cancer Res. 2010;70:9979-90.
42. Maa MC, Lee JC, Chen YJ, Chen YJ, Lee YC, Wang ST, et al. Eps8 facilitates cellular growth and motility of colon cancer cells by increasing the expression and activity of focal adhesion kinase. J Biol Chem. 2007;282:19399-409.
43. Chen C, Liang Z, Huang W, Li X, Zhou F, Hu X, et al. Eps8 regulates cellular proliferation and migration of breast cancer. Int J Oncol. 2015;46:205-14.
44. He YZ, Liang Z, Wu MR, Wen Q, Deng L, Song CY, et al. Overexpression of EPS8 is associated with poor prognosis in patients with acute lymphoblastic leukemia. Leuk Res. 2015;39:575-81.
45. Li Q, Bao W, Fan Q, Shi WJ, Li ZN, Xu Y, et al. Epidermal growth factor receptor kinase substrate 8 promotes the metastasis of cervical cancer via the epithelial-mesenchymal transition. Mol Med Rep. 2016;14:3220-8.

Figure Legends

Figure 1: The functional significance of *miR-130b-5p* and *miR-130b-3p* in PDAC cells.
(A) Expression levels of *miR-130b-5p* and *miR-130b-3p* in PDAC clinical specimens and cell lines (PANC-1 and SW1990). *RNU48* was used as an internal control. (B) Spearman's rank test demonstrated a positive correlation between the expression levels of *miR-130b-5p* and *miR-130b-3p*. (C)-(E) Effects of ectopic expression of *miR-130b-5p* and *miR-130b-3p* on PADC cells. (C) Cell proliferation was determined by XTT assays 72 h following transfection with *miR-130b-5p* or *miR-130b-3p*. (D) Results of cell migration assays. (E) Cell invasion activity was determined using Matrigel invasion assays. *, $p < 0.05$ **, $p < 0.0001$,

Figure 2: Clinical significance of the expression of 9 genes (*EPS8*, *ZWINT*, *SMC4*, *LDHA*, *GJB2*, *ZCCHC24*, *TOP2A*, *ANLN* and *ADCY3*) based on The Cancer Genome Atlas (TCGA) database.
Survival rate differences were analyzed by Kaplan-Meier survival curves and log-rank statistics. (A) Kaplan-Meier plots of overall survival and (B) disease-free survival with log-rank tests for genes with high and low expression from The Cancer Genome Atlas database.

Figure 3: Aberrant expression of *EPS8* in PDAC specimens and its clinical significance
(A) Expression levels of *EPS8* in PDAC clinical specimens. *GUSB* was the internal control. (B) Spearman's rank test was used to evaluate the correlation between *EPS8* expression and *miR-130b-5p* expression in PDAC clinical specimens. (C) Analysis of the expression levels of *EPS8* in patients with PDAC using TCGA database. Forest plot of univariate Cox proportional hazards regression analysis of 5-year overall survival. Univariate and multivariate analyses for OS using TCGA database were carried out by Cox proportional hazards regression analyses. (D) Immunohistochemical analysis of PDAC clinical samples. EPS8 was

strongly expressed in cancer lesions.

Figure 4: Oncogenic function of *EPS8* in PDAC cells.
(A),(B) *miR-130b-5p* directly regulated *EPS8* in PDAC cells. Expression levels of *EPS8* mRNA (A) or EPS8 protein (B) 72 h or 96 h following transfection with 10 nM *miR-130b-5p* into cell lines. (C) *miR-130b-5p* binding site (positions 713-719) in the 3'-UTR of *EPS8* mRNA. Dual luciferase reporter assays using vectors encoding putative *miR-130b-5p* target sites in the *EPS8* 3'-UTRs for both wild-type and deleted regions. *Renilla* luciferase values were normalized to firefly luciferase values. *. $p < 0.005$. (D)-(F) Effects of silencing *EPS8* in PDAC cells. (D) Cell proliferation, (E) migration and (F) invasion assays. These assays showed that inhibition of migration and invasion were observed in si-*EPS8*-transfected cell lines (PANC-1 and SW1990). *, $p < 0.005$.

Supplemental Figure 1: Strategy for identification of putative target genes regulated by *miR-130b-5p* in PDAC cells.
A total of 1,622 and 2,301 genes were downregulated by *miR-130b-5p* transfection into PANC-1 and SW1990 cells, respectively. Among these genes, 103 genes were controlled by *miR-130b-5p* and 40 genes have putative target sites of *miR-130b-5p* by TargetScan database analyses. High expression of 9 genes was significantly associated with poor prognosis of the patients with PDAC by OncoLnc database analyses.

Supplemental Figure 2: Strategy for identification of putative downregulated genes mediated by *EPS8* in PDAC cells.
A total of 697 genes were downregulated by si-*EPS8* transfection into PANC-1 cells. Among these genes, 48 were upregulated in PDAC clinical specimens and 8 genes were closely associated with PDAC prognosis.

Supplemental Figure 3: Both strands of pre-*miR-130b* (*miR-130b-5p*, the passenger strand and *miR-130b-3p*, the guide strand) were

incorporated into RISC. (A) Schematic illustration of miRNA detection methods. Isolation of RISC-incorporated miRNAs by Ago2 immunoprecipitation. (B) Amounts of *miR-130b-5p* or *miR-130b-3p* after transfection with *miR-130b-5p* or *miR-130b-3p*. PCR data were normalized by the expression of *miR-21*. *, $p < 0.005$.

Supplemental Figure 4: Downregulation of *EPS8* mRNA and EPS8 protein expression after si-*EPS8* transfection of PDAC cell lines (PANC-1 and SW1990).
(A) *EPS8* mRNA expression in PDAC cell lines was evaluated by qRT-PCR 72 h after transfection with si-*EPS8*-1 or si-*EPS8*-2. *GUSB* was used as an internal control; data were normalized to *GUSB* expression. *, $p < 0.0001$ (B) EPS8 protein expression in PDAC cell lines was evaluated by Western blot analysis 96 h after transfection with si-*EPS8*-1 or si-*EPS8*-2. GAPDH was used as a loading control.

Supplemental Figure 5: Clinical significance of the expression of 7 genes (*MET*, *HMGA2*, *FERMT1*, *RARRES3*, *PTK2*, *MAD2L1* and *FLI1*) based on The Cancer Genome Atlas (TCGA) database. (A) Kaplan-Meier plots of overall survival and (B) disease-free survival with log-rank tests for genes with high and low expression from The Cancer Genome Atlas database.

Supplemental Figure 6: The sequences and chromosomal locations of *miR-130*-family miRNAs.
(A) Chromosomal locations of *miR-130a*, *miR-130b*, *miR-301a* and *miR-301b*. (B) Mature miRNAs of both strands of pre-miRNA (*miR-130a*, *miR-130b*, *miR-301a* and *miR-301b*) and seed sequences of these miRNAs are shown by underlining.

Table.1 Identification of putative targets regulated by *miR-130b-5p* in PDAC cells

Entrez GeneID	Gene symbol	Gene name	Expression in PANC-1 miR-130b-5p transfectants (FClog2<-1.0)	GEO (FClog2>1.0)	TCGA_OncoLnc OS *p*-value (in 5 years)
2059	*EPS8*	epidermal growth factor receptor pathway substrate 8	-1.0391617	1.2628669	<0.0001
11130	*ZWINT*	ZW10 interacting kinetochore protein	-1.4909135	1.1604217	0.0003
10051	*SMC4*	structural maintenance of chromosomes 4	-1.1281776	1.0477006	0.0015
3939	*LDHA*	lactate dehydrogenase A	-1.0913677	1.2467416	0.0016
2706	*GJB2*	gap junction protein, beta 2, 26kDa	-1.0175266	3.6934876	0.0026
219654	*ZCCHC24*	zinc finger, CCHC domain containing 24	-1.2267109	1.4362591	0.0030
7153	*TOP2A*	topoisomerase (DNA) II alpha 170kDa	-1.7036874	1.5301974	0.0036
54443	*ANLN*	anillin, actin binding protein	-1.3910149	1.7292130	0.0037
109	*ADCY3*	adenylate cyclase 3	-1.0753918	1.0011512	0.0049
9055	*PRC1*	protein regulator of cytokinesis 1	-1.3384857	1.0667097	0.0123
6241	*RRM2*	ribonucleotide reductase M2	-1.3087503	1.1663941	0.0195
55013	*CCDC109B*	coiled-coil domain containing 109B	-1.1029720	1.9479591	0.0226
55601	*DDX60*	DEAD (Asp-Glu-Ala-Asp) box polypeptide 60	-1.5366727	1.5572646	0.0241
3691	*ITGB4*	integrin, beta 4	-1.2837483	1.2316791	0.0292
91404	*SESTD1*	SEC14 and spectrin domains 1	-1.6589893	1.3892033	0.0324
444	*ASPH*	aspartate beta-hydroxylase	-1.1716107	1.4017963	0.0331
2687	*GGT5*	gamma-glutamyltransferase 5	-1.1898923	1.1288950	0.0482
56925	*LXN*	latexin	-1.4351722	2.0470986	0.0493
6772	*STAT1*	signal transducer and activator of transcription 1, 91kDa	-1.6604798	1.5651450	0.0521
26509	*MYOF*	myoferlin	-1.1385632	2.4245954	0.0576
8777	*MPDZ*	multiple PDZ domain protein	-1.2851086	1.0890113	0.0668
26031	*OSBPL3*	oxysterol binding protein-like 3	-1.7567873	1.6363204	0.0713
1601	*DAB2*	Dab, mitogen-responsive phosphoprotein, homolog 2 (Drosophila)	-1.0613184	1.0355528	0.0780
55075	*UACA*	uveal autoantigen with coiled-coil domains and ankyrin repeats	-2.4191770	1.2785207	0.0820
3339	*HSPG2*	heparan sulfate proteoglycan 2	-1.2415609	1.0803752	0.0920
80896	*NPL*	N-acetylneuraminate pyruvate lyase (dihydrodipicolinate synthase)	-1.2635889	1.6554387	0.0950
79718	*TBL1XR1*	transducin (beta)-like 1 X-linked receptor 1	-1.2307795	1.0184109	0.0983
9749	*PHACTR2*	phosphatase and actin regulator 2	-1.9079069	1.0210196	0.1046
2745	*GLRX*	glutaredoxin (thioltransferase)	-1.4243727	1.2816241	0.1083
5954	*RCN1*	reticulocalbin 1, EF-hand calcium binding domain	-1.2084924	1.4771140	0.1103
79026	*AHNAK*	AHNAK nucleoprotein	-1.3486654	1.0858593	0.1105
4628	*MYH10*	myosin, heavy chain 10, non-muscle	-1.0401611	1.1421649	0.1230
2115	*ETV1*	ets variant 1	-1.0961652	2.3057034	0.1239
51316	*PLAC8*	placenta-specific 8	-1.7858686	1.6964420	0.1257
5357	*PLS1*	plastin 1	-1.0227555	1.1227326	0.1294
54933	*RHBDL2*	rhomboid, veinlet-like 2 (Drosophila)	-1.4695596	1.1792967	0.1424
145389	*SLC38A6*	solute carrier family 38, member 6	-1.2434853	1.4723484	0.1577
54492	*NEURL1B*	neuralized E3 ubiquitin protein ligase 1B	-1.2289410	1.2359435	0.1680
1687	*DFNA5*	deafness, autosomal dominant 5	-2.4118986	1.3480556	0.1707
5159	*PDGFRB*	platelet-derived growth factor receptor, beta polypeptide	-1.6300844	1.7990630	0.1902
5738	*PTGFRN*	prostaglandin F2 receptor inhibitor	-1.1871296	1.4020885	0.1939
4093	*SMAD9*	SMAD family member 9	-1.0708561	1.1712591	0.2192
57182	*ANKRD50*	ankyrin repeat domain 50	-1.5082961	1.2401948	0.2229
3696	*ITGB8*	integrin, beta 8	-1.1564417	1.5737898	0.2358
3434	*IFIT1*	interferon-induced protein with tetratricopeptide repeats 1	-1.5218506	1.2770477	0.2408
399474	*TMEM200B*	transmembrane protein 200B	-2.0416780	1.0096044	0.2464
57674	*RNF213*	ring finger protein 213	-2.5736365	1.4979298	0.2474
64754	*SMYD3*	SET and MYND domain containing 3	-1.0121193	1.1509621	0.2509
57157	*PHTF2*	putative homeodomain transcription factor 2	-1.4924613	1.3032500	0.2571
84441	*MAML2*	mastermind-like 2 (Drosophila)	-1.3098994	1.3333797	0.2598
1311	*COMP*	cartilage oligomeric matrix protein	-1.1994047	3.5716603	0.2606
401494	*PTPLAD2(HACD4)*	protein tyrosine phosphatase-like A domain containing 2	-1.0844336	1.5488394	0.2682
5552	*SRGN*	serglycin	-1.4376887	1.4919588	0.2782
130271	*PLEKHH2*	pleckstrin homology domain containing, family H (with MyTH4 domain) member 2	-2.2517653	1.2622999	0.2824
441168	*FAM26F*	family with sequence similarity 26, member F	-1.0591393	1.1706267	0.2829
5176	*SERPINF1*	serpin peptidase inhibitor, clade F (alpha-2 antiplasmin, pigment epithelium derived factor), member 1	-1.0058947	1.3390279	0.3265
29969	*MDFIC*	MyoD family inhibitor domain containing	-1.4263206	1.2081294	0.3845
3433	*IFIT2*	interferon-induced protein with tetratricopeptide repeats 2	-1.3565645	1.4609243	0.3916
7046	*TGFBR1*	transforming growth factor, beta receptor 1	-1.7564989	1.5672281	0.4061
9638	*FEZ1*	fasciculation and elongation protein zeta 1 (zygin	-1.3657641	1.1956161	0.4099
10403	*NDC80*	NDC80 kinetochore complex component	-1.2600021	1.5473172	0.4113
259232	*NALCN*	sodium leak channel, non selective	-2.0426240	1.7215563	0.4212
7464	*CORO2A*	coronin, actin binding protein, 2A	-1.1782600	1.0355257	0.4377
10687	*PNMA2*	paraneoplastic Ma antigen 2	-1.2503138	2.0604417	0.4674
114882	*OSBPL8*	oxysterol binding protein-like 8	-1.2117767	1.0806354	0.4699
3912	*LAMB1*	laminin, beta 1	-1.1625280	1.6784895	0.4837
29887	*SNX10*	sorting nexin 10	-1.1817684	1.2034102	0.4885
4053	*LTBP2*	latent transforming growth factor beta binding protein 2	-1.1001697	1.7000597	0.4888
57333	*RCN3*	reticulocalbin 3, EF-hand calcium binding domain	-1.0096655	1.2093748	0.5065
57480	*PLEKHG1*	pleckstrin homology domain containing, family G (with RhoGef domain) member 1	-1.3316975	1.5672085	0.5090
493869	*GPX8*	glutathione peroxidase 8 (putative)	-2.4862900	2.1368702	0.5220
1122	*CHML*	choroideremia-like (Rab escort protein 2)	-1.4233093	1.2285766	0.5285
8829	*NRP1*	neuropilin 1	-1.4793081	1.3021802	0.5412
8819	*SAP30*	Sin3A-associated protein, 30kDa	-1.0623255	1.0942839	0.5456
83879	*CDCA7*	cell division cycle associated 7	-1.2634476	1.3187604	0.5659
4921	*DDR2*	discoidin domain receptor tyrosine kinase 2	-1.0453687	1.4877484	0.5667
80328	*ULBP2*	UL16 binding protein 2	-2.3729725	1.2354260	0.5685
10123	*ARL4C*	ADP-ribosylation factor-like 4C	-1.2759942	2.2831240	0.5705
55711	*FAR2*	fatty acyl CoA reductase 2	-1.2279121	1.0489434	0.5748
25878	*MXRA5*	matrix-remodelling associated 5	-1.1647496	2.3869526	0.5751
162073	*ITPRIPL2*	inositol 1,4,5-trisphosphate receptor interacting protein-like 2	-1.3766663	1.0587933	0.6025
8321	*FZD1*	frizzled class receptor 1	-1.7407991	1.1861601	0.6113
6443	*SGCB*	sarcoglycan, beta (43kDa dystrophin-associated glycoprotein)	-1.4844265	1.1196231	0.6616
23092	*ARHGAP26*	Rho GTPase activating protein 26	-1.8215991	1.4714981	0.6710
4815	*NINJ2*	ninjurin 2	-1.2982117	1.1460175	0.6778
30011	*SH3KBP1*	SH3-domain kinase binding protein 1	-1.3079715	1.6522795	0.6995
4175	*MCM6*	minichromosome maintenance complex component 6	-1.0063353	1.0153162	0.7117
5911	*RAP2A*	RAP2A, member of RAS oncogene family	-1.1328840	1.0579273	0.7322
9902	*MRC2*	mannose receptor, C type 2	-1.0907621	1.3853211	0.7776
133418	*EMB*	embigin	-1.1111135	1.4472933	0.7843
84168	*ANTXR1*	anthrax toxin receptor 1	-1.1164263	2.9024701	0.8002
1287	*COL4A5*	collagen, type IV, alpha 5	-1.1768475	1.1700162	0.8029
8082	*SSPN*	sarcospan	-1.5962458	1.1331555	0.8072
8543	*LMO4*	LIM domain only 4	-1.3773192	1.0676418	0.8208
10551	*AGR2*	anterior gradient 2	-1.2424725	2.0485048	0.8335
23271	*CAMSAP2*	calmodulin regulated spectrin-associated protein family, member 2	-1.0790195	1.3784356	0.8550
8324	*FZD7*	frizzled class receptor 7	-1.4669601	1.5851643	0.8594
4286	*MITF*	microphthalmia-associated transcription factor	-1.6427531	1.1172881	0.8612
1475	*CSTA*	cystatin A (stefin A)	-1.5165935	2.0940666	0.8674
90459	*ERI1*	exoribonuclease 1	-1.2428759	1.0876643	0.8894
1296	*COL8A2*	collagen, type VIII, alpha 2	-1.4797236	1.9936453	0.9346
80005	*DOCK5*	dedicator of cytokinesis 5	-1.0028888	1.2031072	0.9558
150759	*LINC00342*	long intergenic non-protein coding RNA 342	-1.1021174	1.4145094	-

Table.2 Identification of *EPS8* mediated downstream genes in PDAC cells

Entrez GeneID	Gene symbol	Gene name	Expression in PANC-1 si-*EPS8* transfectants (FClog2<-1.0)	GEO (FClog2>1.0)	TCGA_OncoLnc OS *p*-value (in 5 years)
2059	*EPS8*	epidermal growth factor receptor pathway substrate 8	-2.8271956	2.3997214	<0.0001
4233	*MET*	MET proto-oncogene, receptor tyrosine kinase	-1.0782841	2.8329950	0.0015
8091	*HMGA2*	high mobility group AT-hook 2	-2.3884200	2.4964874	0.0031
55612	*FERMT1*	fermitin family member 1	-1.3296491	3.1556027	0.0103
5920	*RARRES3*	retinoic acid receptor responder (tazarotene induced) 3	-1.1847581	2.8853405	0.0125
5747	*PTK2*	protein tyrosine kinase 2	-1.0931424	2.1476655	0.0134
4085	*MAD2L1*	MAD2 mitotic arrest deficient-like 1 (yeast)	-1.3218220	2.2757983	0.0412
2313	*FLI1*	Fli-1 proto-oncogene, ETS transcription factor	-1.2141428	2.1929195	0.0443
3437	*IFIT3*	interferon-induced protein with tetratricopeptide repeats 3	-2.7479300	2.5652308	0.0574
84034	*EMILIN2*	elastin microfibril interfacer 2	-2.3441610	2.3126762	0.0868
3397	*ID1*	inhibitor of DNA binding 1, dominant negative helix-loop-helix	-1.2009468	2.4448597	0.0969
79026	*AHNAK*	AHNAK nucleoprotein	-1.3035727	2.1226394	0.1105
54739	*XAF1*	XIAP associated factor 1	-1.2250342	3.6524053	0.1327
7764	*ZNF217*	zinc finger protein 217	-1.0156298	2.1386855	0.1358
6286	*S100P*	S100 calcium binding protein P	-1.7940164	12.7159950	0.1515
6001	*RGS10*	regulator of G-protein signaling 10	-1.3992062	3.0485551	0.1700
5159	*PDGFRB*	platelet-derived growth factor receptor, beta polypeptide	-2.2982244	3.4799414	0.1902
7220	*TRPC1*	transient receptor potential cation channel, subfamily C, member 1	-1.0543852	2.8364346	0.1999
23603	*CORO1C*	coronin, actin binding protein, 1C	-1.8096170	2.9602175	0.2026
330	*BIRC3*	baculoviral IAP repeat containing 3	-1.5710629	2.6069708	0.2322
3434	*IFIT1*	interferon-induced protein with tetratricopeptide repeats 1	-1.2829789	2.4234254	0.2408
57674	*RNF213*	ring finger protein 213	-2.2830563	2.8243713	0.2474
3915	*LAMC1*	laminin, gamma 1 (formerly LAMB2)	-1.0173159	2.5432700	0.2490
659	*BMPR2*	bone morphogenetic protein receptor, type II (serine/threonine kinase)	-2.0797455	2.4564056	0.3162
716	*C1S*	complement component 1, s subcomponent	-1.3375945	4.1859550	0.3696
7498	*XDH*	xanthine dehydrogenase	-1.0785036	2.2759452	0.3800
29969	*MDFIC*	MyoD family inhibitor domain containing	-1.1913158	2.3103788	0.3845
3433	*IFIT2*	interferon-induced protein with tetratricopeptide repeats 2	-2.7081504	2.7528467	0.3916
7046	*TGFBR1*	transforming growth factor, beta receptor 1	-1.0406232	2.7592096	0.4061
259232	*NALCN*	sodium leak channel, non selective	-1.8967161	3.2979198	0.4212
64859	*NABP1*	nucleic acid binding protein 1	-1.0262889	2.4854288	0.4593
29887	*SNX10*	sorting nexin 10	-1.0249023	2.3028336	0.4885
219285	*SAMD9L*	sterile alpha motif domain containing 9-like	-1.2528054	2.2927480	0.5013
6453	*ITSN1*	intersectin 1 (SH3 domain protein)	-1.0911493	2.3252943	0.5098
253782	*CERS6*	ceramide synthase 6	-1.2245360	2.0965688	0.5536
727936	*GXYLT2*	glucoside xylosyltransferase 2	-2.9657586	4.1614670	0.5649
9120	*SLC16A6*	solute carrier family 16, member 6	-1.0826521	2.3125410	0.5799
1953	*MEGF6*	multiple EGF-like-domains 6	-1.4605589	2.2775905	0.5966
26064	*RAI14*	retinoic acid induced 14	-1.4694735	2.7101336	0.6374
6016	*RIT1*	Ras-like without CAAX 1	-1.1128588	2.2873511	0.6606
4026	*LPP*	LIM domain containing preferred translocation partner in lipoma	-1.3406305	2.0011916	0.7361
1728	*NQO1*	NAD(P)H dehydrogenase, quinone 1	-1.2154182	4.5524726	0.8302
59339	*PLEKHA2*	pleckstrin homology domain containing, family A (phosphoinositide binding specific) member 2	-1.5718870	2.0061517	0.8335
1871	*E2F3*	E2F transcription factor 3	-1.0145493	2.4384596	0.8898
397	*ARHGDIB*	Rho GDP dissociation inhibitor (GDI) beta	-1.5170516	3.2517672	0.9057
10365	*KLF2*	Kruppel-like factor 2	-1.7209059	2.0431898	0.9088
51056	*LAP3*	leucine aminopeptidase 3	-1.7265989	2.0905375	0.9187
1296	*COL8A2*	collagen, type VIII, alpha 2	-1.0540862	3.9824197	0.9346

JHG Figure 1

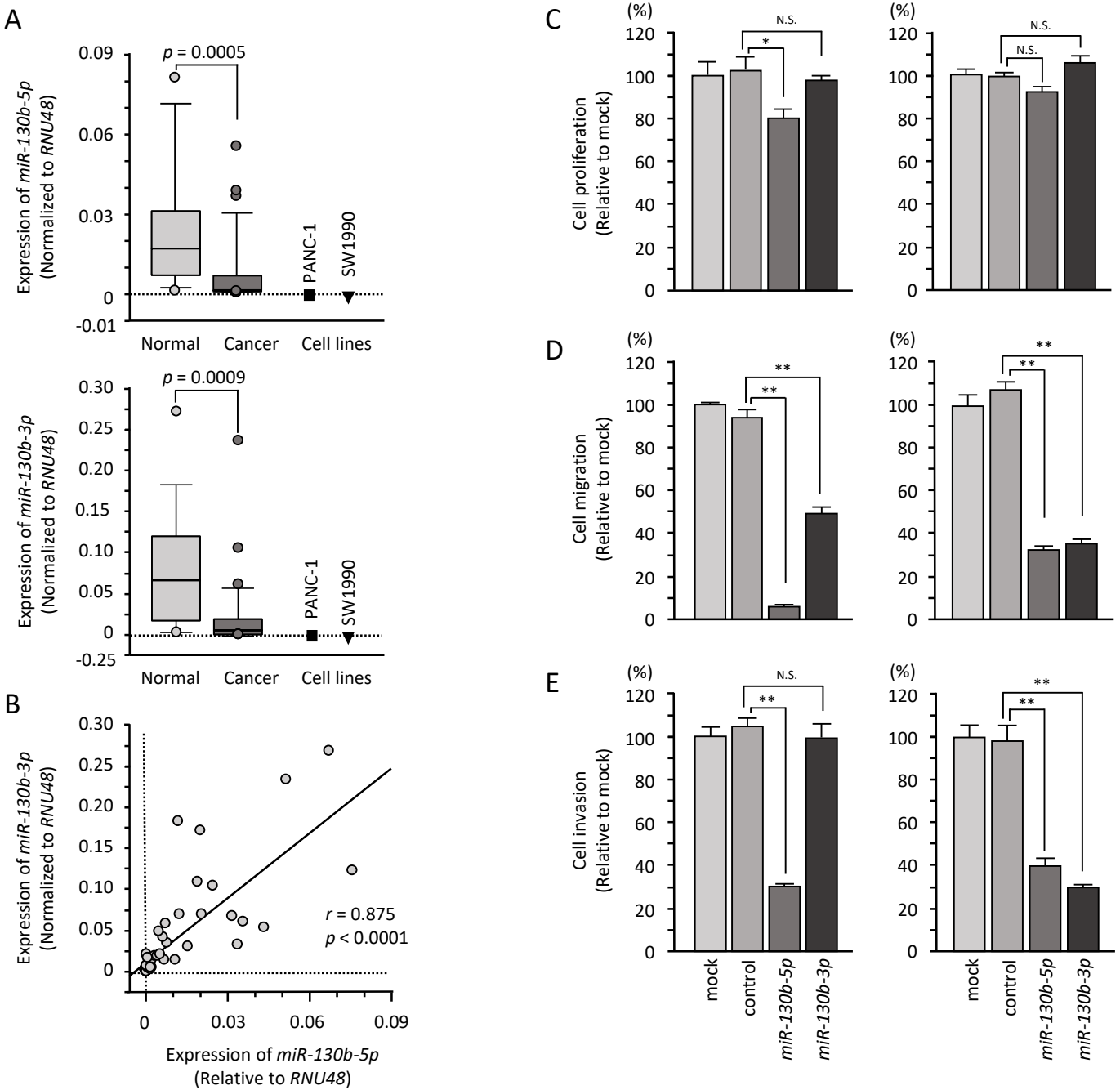
A
p = 0.0005
Expression of miR-130b-5p (Normalized to RNU48)
0.09
0.06
0.03
0
-0.01
PANC-1
SW1990
Normal
Cancer
Cell lines
p = 0.0009
Expression of miR-130b-3p (Normalized to RNU48)
0.30
0.25
0.20
0.15
0.10
0.05
0
-0.25
B
r = 0.875
p < 0.0001
Expression of miR-130b-5p (Relative to RNU48)
C
PANC-1
SW1990
Cell proliferation (Relative to mock)
(%)
N.S.
*
D
Cell migration (Relative to mock)
**
E
Cell invasion (Relative to mock)
mock
control
miR-130b-5p
miR-130b-3p

JHG Figure 2

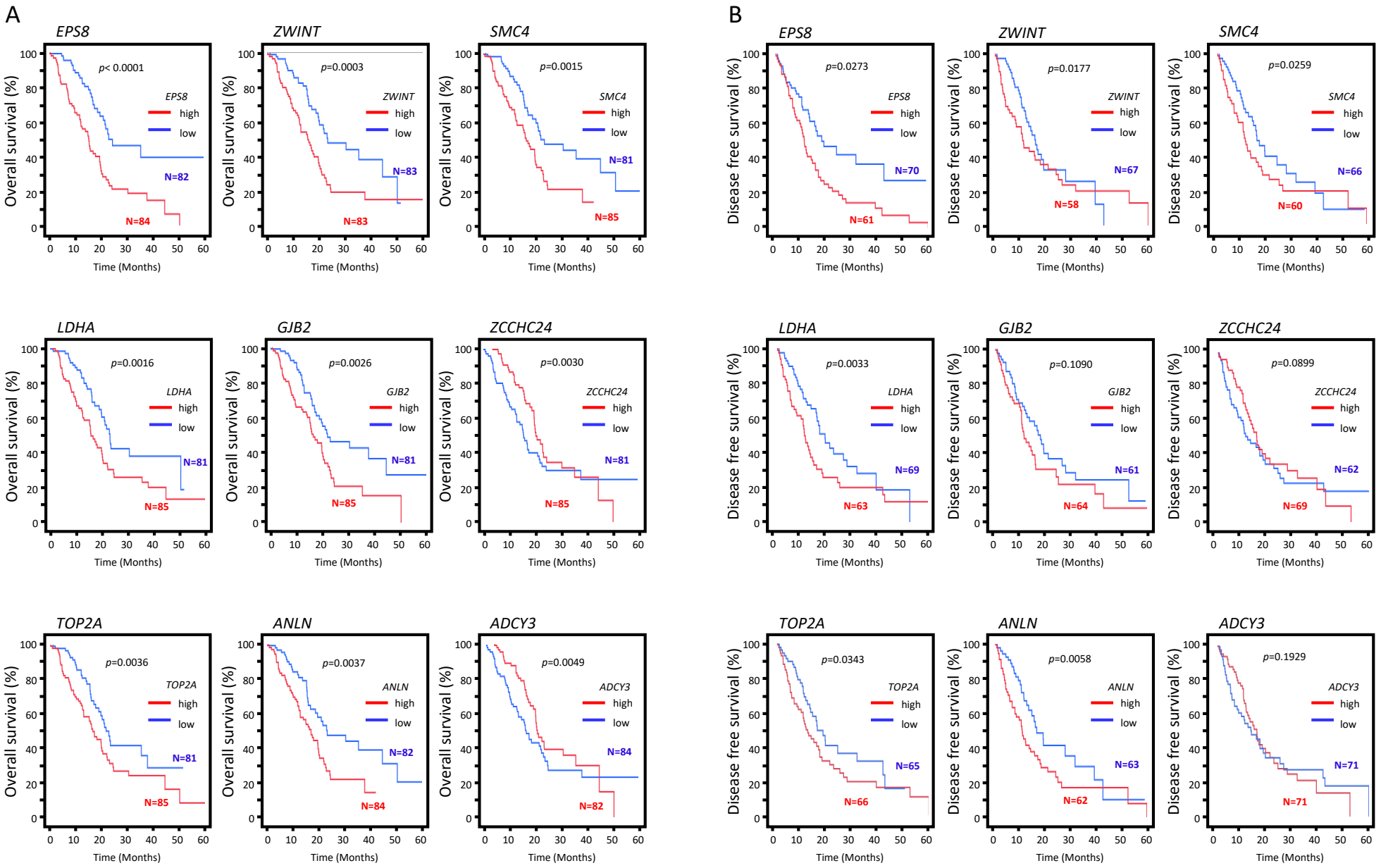
A
EPS8
p< 0.0001
high
low
N=82
N=84
Overall survival (%)
Time (Months)
ZWINT
p=0.0003
N=83
N=83
SMC4
p=0.0015
N=81
N=85
LDHA
p=0.0016
N=81
N=85
GJB2
p=0.0026
N=81
N=85
ZCCHC24
p=0.0030
N=81
N=85
TOP2A
p=0.0036
N=81
N=85
ANLN
p=0.0037
N=82
N=84
ADCY3
p=0.0049
N=84
N=82
B
Disease free survival (%)
p=0.0273
N=70
N=61
p=0.0177
N=67
N=58
p=0.0259
N=66
N=60
p=0.0033
N=69
N=63
p=0.1090
N=61
N=64
p=0.0899
N=62
N=69
p=0.0343
N=65
N=66
p=0.0058
N=63
N=62
p=0.1929
N=71
N=71

JHG Figure 3

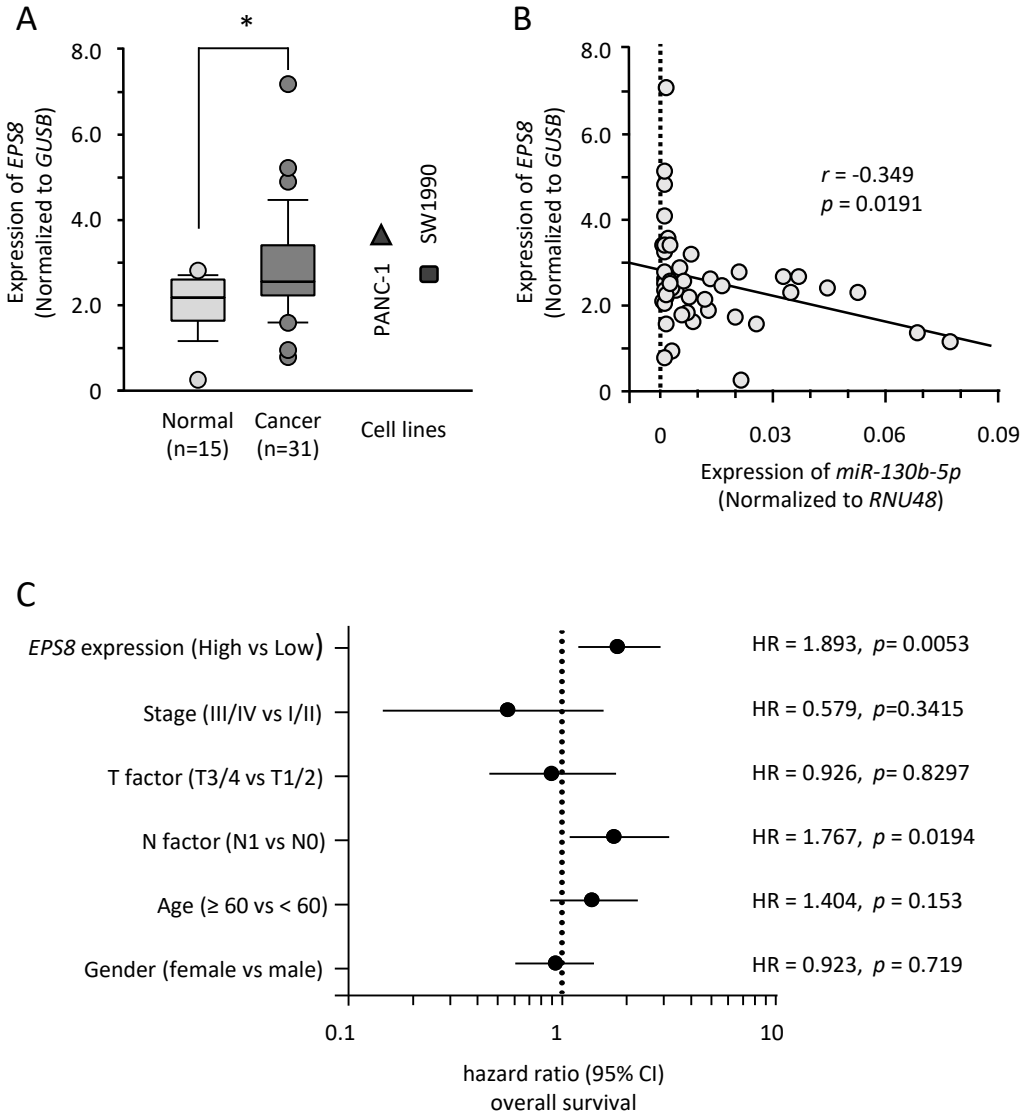
A
*
8.0
6.0
4.0
2.0
0
Expression of EPS8
(Normalized to GUSB)
PANC-1
SW1990
Normal
(n=15)
Cancer
(n=31)
Cell lines
B
8.0
6.0
4.0
2.0
0
Expression of EPS8
(Normalized to GUSB)
r = -0.349
p = 0.0191
0
0.03
0.06
0.09
Expression of miR-130b-5p
(Normalized to RNU48)
C
EPS8 expression (High vs Low)
Stage (III/IV vs I/II)
T factor (T3/4 vs T1/2)
N factor (N1 vs N0)
Age (≥ 60 vs < 60)
Gender (female vs male)
HR = 1.893, p= 0.0053
HR = 0.579, p=0.3415
HR = 0.926, p= 0.8297
HR = 1.767, p = 0.0194
HR = 1.404, p = 0.153
HR = 0.923, p = 0.719
0.1
1
10
hazard ratio (95% CI)
overall survival
D
Tumor 9
×200
Tumor 17
×200
Tumor 27
×200

JHG Figure 4

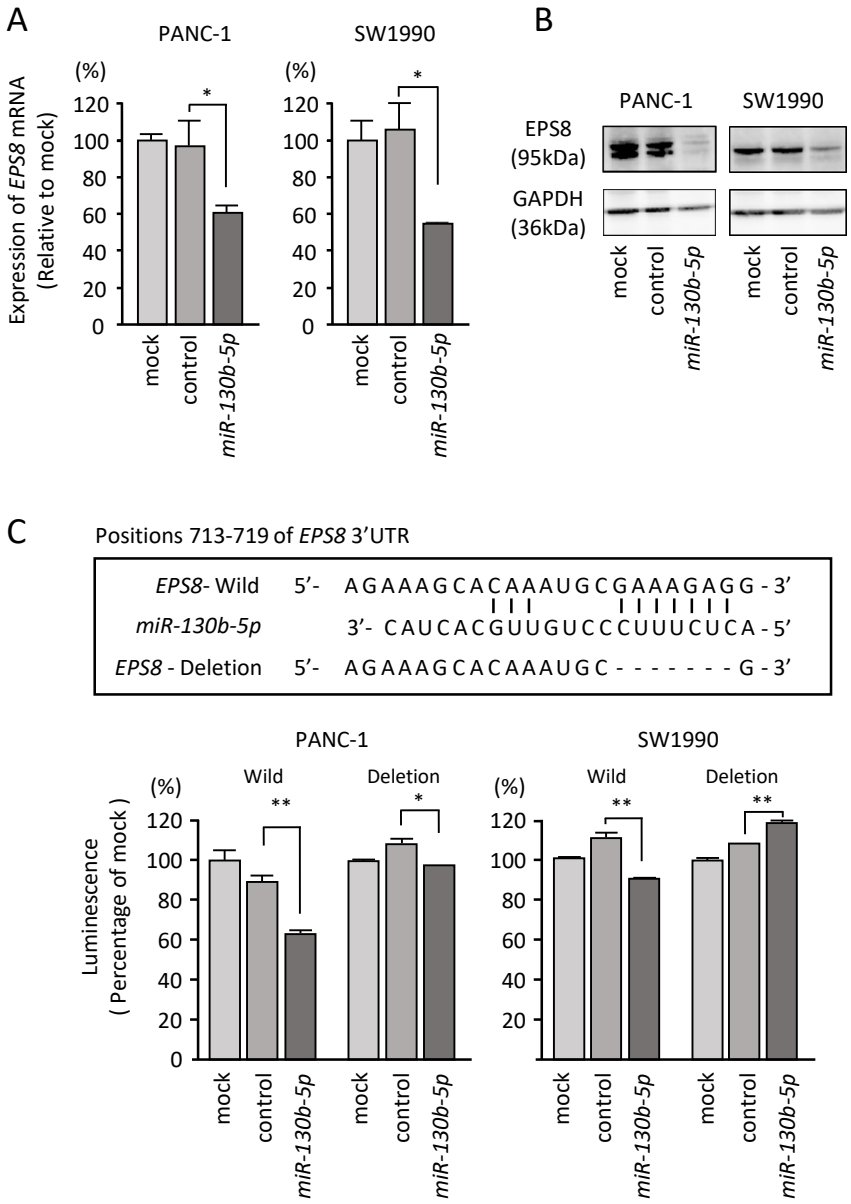
A
PANC-1
SW1990
Expression of EPS8 mRNA (Relative to mock)
(%)
mock
control
miR-130b-5p
B
PANC-1
SW1990
EPS8 (95kDa)
GAPDH (36kDa)
C
Positions 713-719 of EPS8 3'UTR
EPS8- Wild 5'- AGAAAGCACAAAUGCGAAAGAGG - 3'
miR-130b-5p 3'- CAUCACGUUGUCCCUUUCUCA - 5'
EPS8 - Deletion 5'- AGAAAGCACAAAUGC - - - - - - - G - 3'
Luminescence (Percentage of mock)
Wild
Deletion
D
Cell proliferation (Relative to mock)
N.S.
E
Cell migration (Relative to mock)
F
Cell invasion (Relative to mock)
si-EPS8-1
si-EPS8-2

Supplemental Table.1A Clinical samples patient characteristics

No.	Age	Sex	Location	T	N	M	stage	Differentiation
Tumor 1	42	M	pancreas head	3	1	0	2B	well-moderate
Tumor 2	44	M	pancreas head	3	1	0	2B	modetrate
Tumor 3	76	M	pancreas head	3	1	0	2B	mode-poor
Tumor 4	67	M	pancreas head	3	1	0	2B	moderate
Tumor 5	78	F	pancreas head	3	0	0	2A	Papillary
Tumor 6	66	M	pancreas head	3	1	0	2B	moderate
Tumor 7	58	F	pancreas head	3	0	0	2A	moderate
Tumor 8	42	F	pancreas head	3	1	0	2B	well
Tumor 9	65	M	pancreas body	3	1	1	4	well
Tumor 10	56	F	pancreas body	3	1	0	2B	well
Tumor 11	79	F	pancreas head	1	0	0	1A	well
Tumor 12	70	M	pancreas head	3	1	0	2B	well
Tumor 13	63	F	pancreas head	3	0	0	2A	poor
Tumor 14	52	M	pancreas body	3	1	0	2B	well
Tumor 15	56	M	pancreas body	3	1	1	4	well
Tumor 16	65	M	pancreas body	2	0	0	1B	well
Tumor 17	78	F	pancreas head	3	1	0	2B	well+poor
Tumor 18	50	F	pancreas head	3	0	1	4	neuro
Tumor 19	66	F	pancreas head	3	0	0	2A	well
Tumor 20	66	F	pancreas head	3	1	0	2B	well+poor
Tumor 21	67	M	pancreas tail	0	0	0	0	no date
Tumor 22	74	M	pancreas tail	3	0	0	2A	well
Tumor 23	70	F	pancreas body	3	1	0	2B	well+mucosa
Tumor 24	74	F	pancreas body	3	1	0	2B	well
Tumor 25	65	F	pancreas head	3	1	0	2B	well+poor
Tumor 26	78	M	pancreas head	3	0	0	2A	well
Tumor 27	76	M	pancreas head	3	1	0	2B	moderate
Tumor 28	75	M	pancreas head	3	1	0	2B	poor
Tumor 29	71	F	pancreas body	3	0	0	2A	well+poor
Tumor 30	64	M	pancreas head	3	0	0	2A	moderate
Tumor 31	72	F	pancreas tail	3	1	0	2B	moderate

Supplemental Table.1B Features of patients in noncancerous pancreatic tissues.

No.	Age	Sex
Normal 1	65	F
Normal 2	58	F
Normal 3	77	F
Normal 4	67	M
Normal 5	42	F
Normal 6	71	F
Normal 7	60	M
Normal 8	56	F
Normal 9	67	M
Normal 10	85	F
Normal 11	66	F
Normal 12	65	F
Normal 13	63	M
Normal 14	64	M
Normal 15	72	F

Supplemental Table.2 Common putative 9 target genes their *p*−value is smaller than 0.01

Entrez GeneID	Gene symbol	Gene name	Expression in PANC-1 miR-130b-5p transfectants (FClog2<−1.0)	GEO (FClog2>1.0)	*TCGA_OncoLnc OS *p*−value (in 5 years)	TCGA_OncoLnc DFS *p*−value (in 5 years)
2059	*EPS8*	epidermal growth factor receptor pathway substrate 8	−1.0391617	1.262866923	0.0001	0.0273
11130	*ZWINT*	ZW10 interacting kinetochore protein	−1.4909135	1.160421740	0.0003	0.0177
10051	*SMC4*	structural maintenance of chromosomes 4	−1.1281776	1.047700587	0.0015	0.0259
3939	*LDHA*	lactate dehydrogenase A	−1.0913677	1.246741586	0.0016	0.0033
2706	*GJB2*	gap junction protein, beta 2, 26kDa	−1.0175266	3.693487627	0.0026	0.109
219654	*ZCCHC24*	zinc finger, CCHC domain containing 24	−1.2267109	1.436259135	0.0030	0.0899
7153	*TOP2A*	topoisomerase (DNA) II alpha 170kDa	−1.7036874	1.530197372	0.0036	0.0343
54443	*ANLN*	anillin, actin binding protein	−1.3910149	1.729212966	0.0037	0.0058
109	*ADCY3*	adenylate cyclase 3	−1.0753918	1.001151172	0.0049	0.1929

*p−value<0.01

Supplemental Table.3 Target genes keep conserved sites for miR-130b-5p and highly expressed in PDAC

Entrez GeneID	Gene symbol	Conserved sites				GEO (FClog2>1.0)	*TCGA_OncoLnc OS *p*-value (in 5 years)	TCGA_OncoLnc DFS *p*-value (in 5 years)
		8mer	7mer-m8	7mer-A1	Total			
2059	*EPS8*	0	1	2	3	1.262866923	0.0001	0.0273
219654	*ZCCHC24*	0	0	2	2	1.436259135	0.0030	0.0899
7153	*TOP2A*	0	0	1	1	1.530197372	0.0036	0.0343

*p-value<0.01

Supplemental Table.4 Downregurated 8 genes their p-value is smaller than 0.05 in si-*EPS8* transfected PANC-1 cells

Entrez GeneID	Gene symbol	Gene name	Expression in PANC-1 si-*EPS8* transfectants (FClog2<-1.0)	GEO (FClog2>1.0)	*TCGA_OncoLnc OS *p*-value (in 5 years)	TCGA_OncoLnc DFS p-value (in 5 years)
2059	*EPS8*	epidermal growth factor receptor pathway substrate 8	-2.8271956	2.3997214	0.0001	0.0273
4233	*MET*	MET proto-oncogene, receptor tyrosine kinase	-1.0782841	2.8329950	0.0015	0.0107
8091	*HMGA2*	high mobility group AT-hook 2	-2.3884200	2.4964874	0.0031	0.0060
55612	*FERMT1*	fermitin family member 1	-1.3296491	3.1556027	0.0103	0.0255
5920	*RARRES3*	retinoic acid receptor responder (tazarotene induced) 3	-1.1847581	2.8853405	0.0125	0.0775
5747	*PTK2*	protein tyrosine kinase 2	-1.0931424	2.1476655	0.0134	0.3706
4085	*MAD2L1*	MAD2 mitotic arrest deficient-like 1 (yeast)	-1.3218220	2.2757983	0.0412	0.1125
2313	*FLI1*	Fli-1 proto-oncogene, ETS transcription factor	-1.2141428	2.1929195	0.0443	0.1302

*p-value<0.05

JHG Supplemental Figure 1

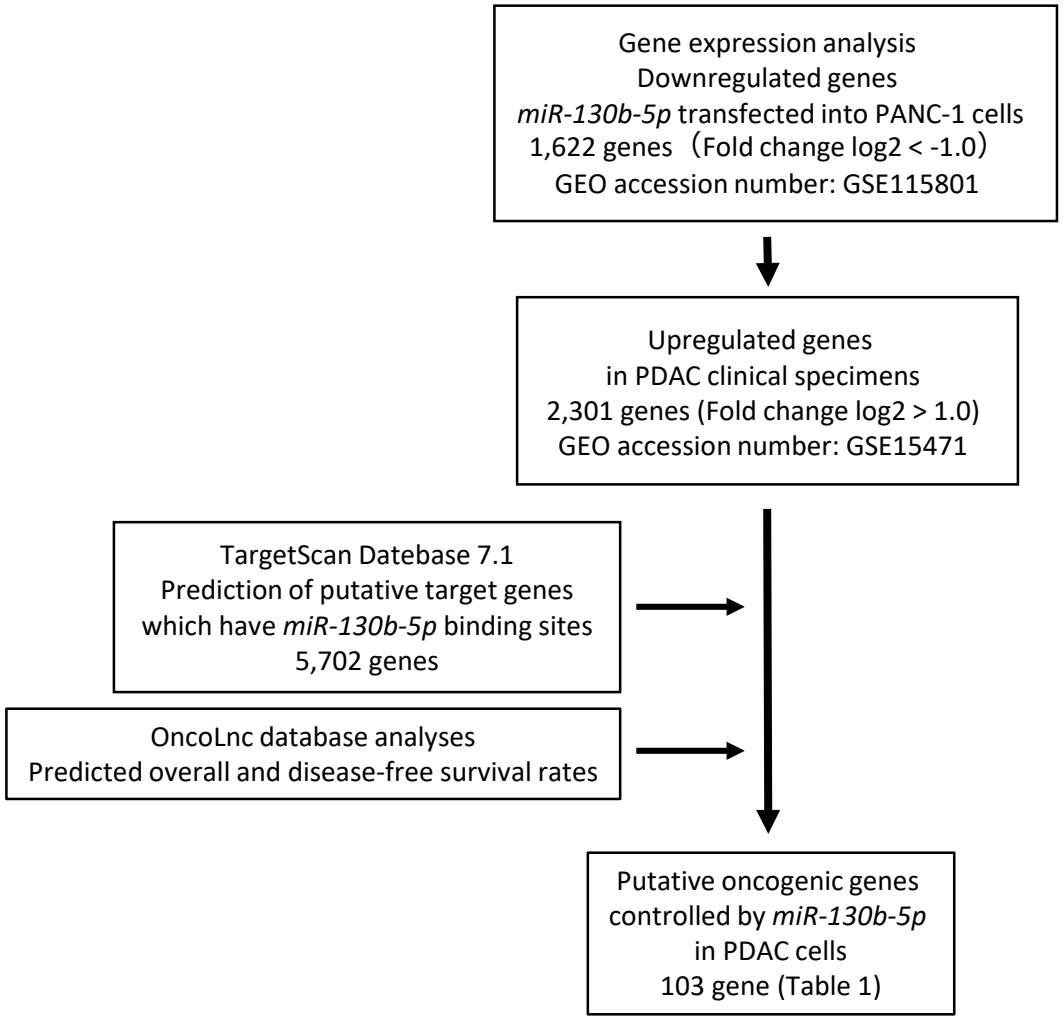

JHG Supplemental Figure 2

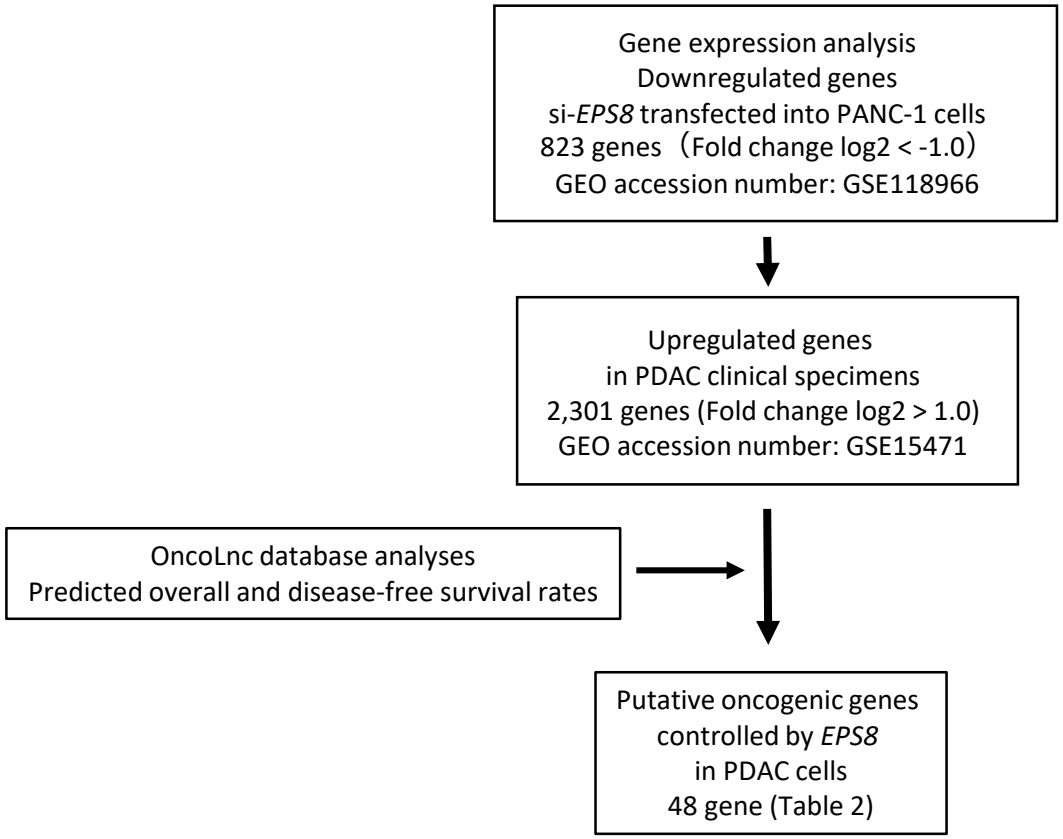

JHG Supplemental Figure 3

A

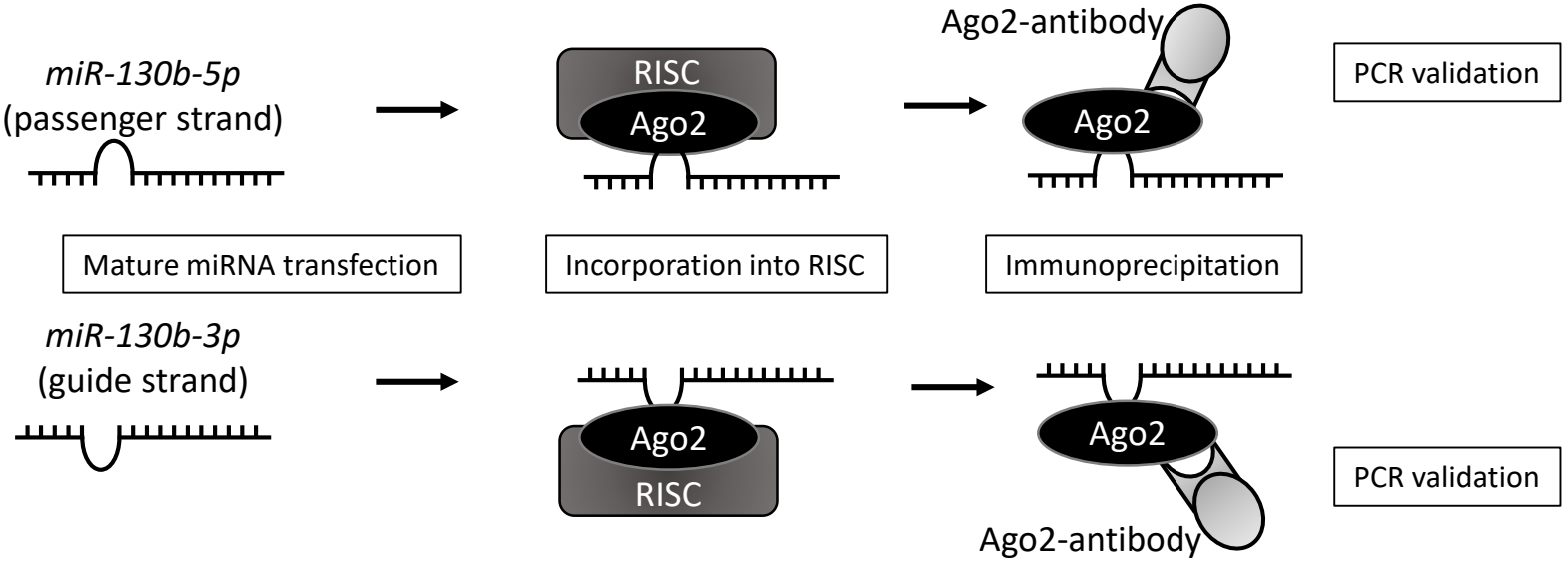

B

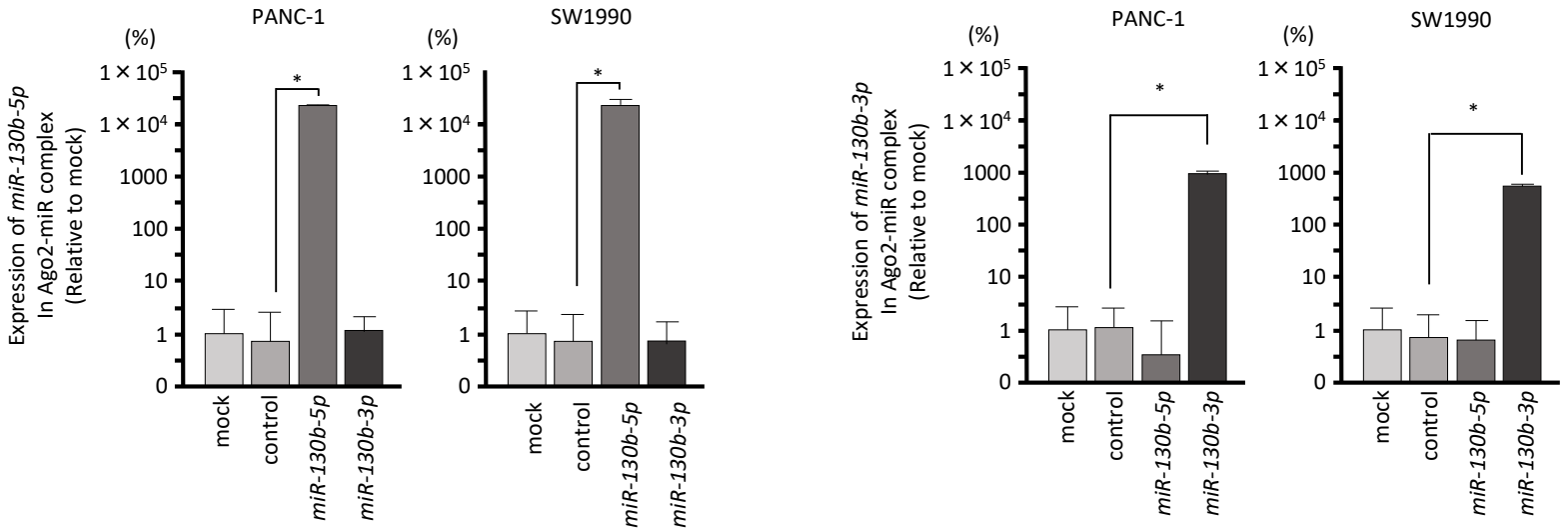

JHG Supplemental Figure 4

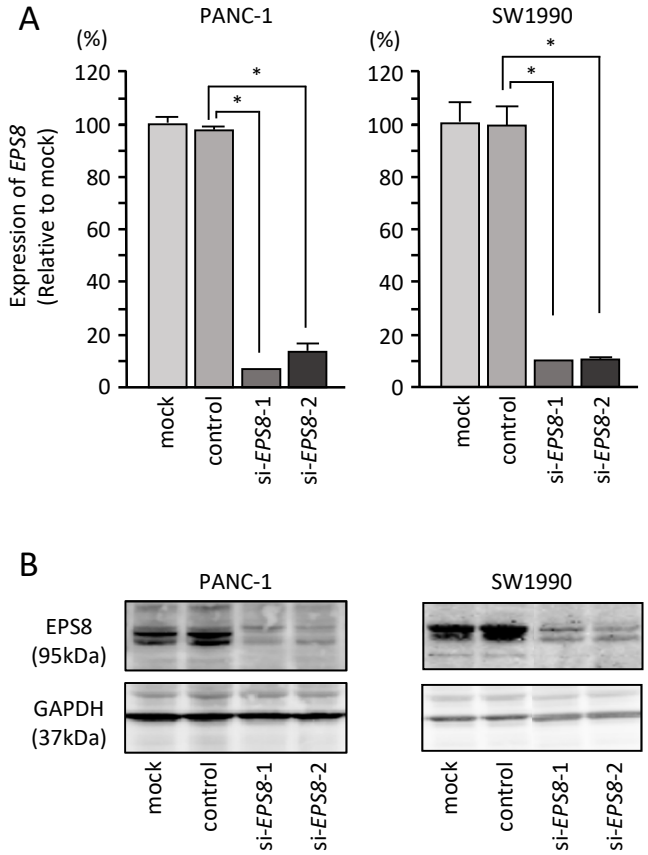

JHG Supplemental Figure 5

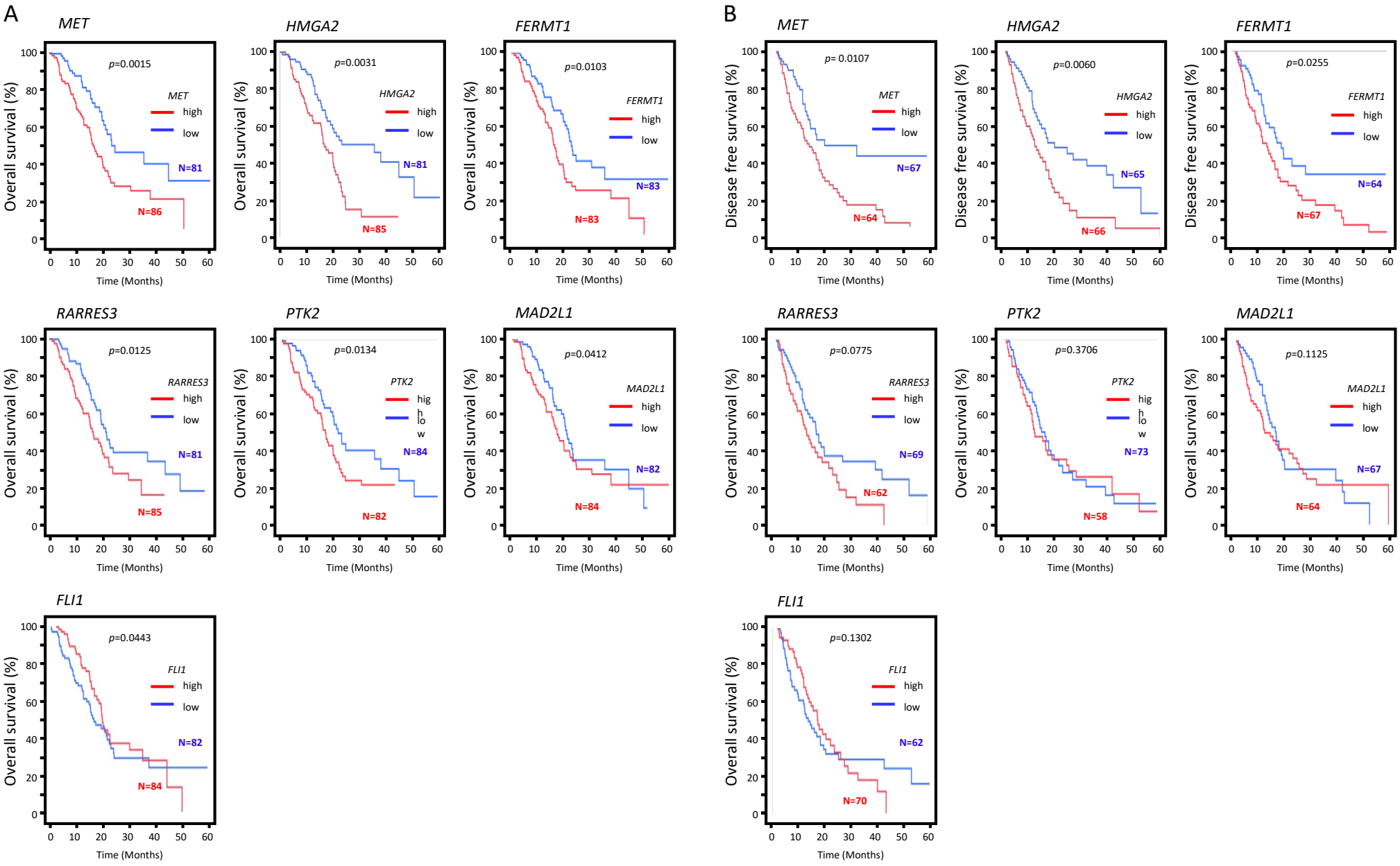

JHG Supplemental Figure 6

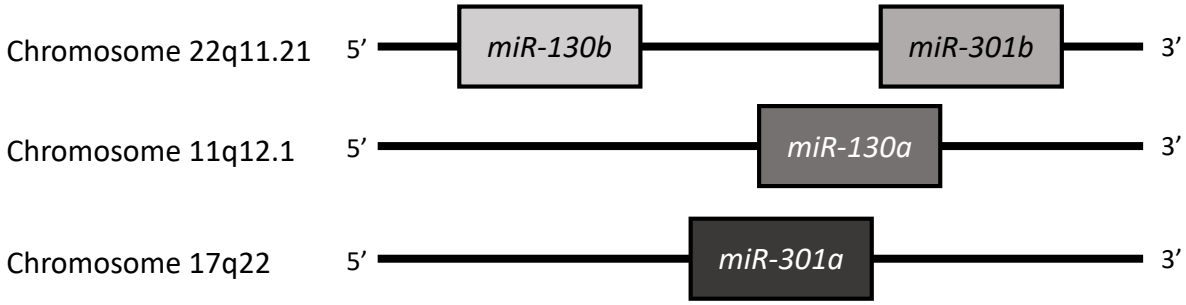

Seed sequences

miR-130b-3p	5'-C AGUGCAA UGAUGAAAGGGCAU-3'
miR-130a-3p	5'-C AGUGCAA UGUUAAAAGGGCAU-3'
miR-301b-3p	5'-C AGUGCAA UGAUAUUGUCAAAGC-3'
miR-301a-3p	5'-C AGUGCAA UAGUAUUGUCAAAGC-3'
miR-130b-5p	5'-A CUCUUUC CCUGUUGCACUAC-3'
miR-130a-5p	5'-G CUCUUUU CACAUUGUGCUACU-3'
miR-301b-5p	5'-G CUCUGAC GAGGUUGCACUACU-3'
miR-301a-5p	5'-G CUCUGAC UUUAUUGCACUACU-3'